

Mechanism Regulating Ca^{2+} -dependent Mechanosensory Behaviour in Sea Urchin Spermatozoa

Yuka Kambara¹, Kogiku Shiba^{2†}, Manabu Yoshida², Chihiro Sato³, Ken Kitajima³, and Chikako Shingyoji^{1*}

¹Department of Biological Sciences, Graduate School of Science, University of Tokyo, Hongo, Tokyo 113-0033, Japan, ²Misaki Marine Biological Station, Graduate School of Science, University of Tokyo, Miura, Kanagawa 238-0225, Japan, ³Bioscience and Biotechnology Center, Nagoya University, Nagoya 464-8601, Japan

ABSTRACT. Flagellar movement of the sea urchin sperm is regulated by intracellular Ca^{2+} . Flagelliasialin, a polysialic acid-containing glycoprotein, as well as other membrane proteins seems responsible for the Ca^{2+} control. To elucidate the mechanism of Ca^{2+} dynamics underlying flagellar movement, we analysed the sperm's mechanosensory behavioural responses by using microtechniques. In sea water containing 10 mM Ca^{2+} , the sperm swim in circular paths. When a mechanical stimulus was applied to the sperm head with a glass microstylus, the sperm showed a series of flagellar responses, consisting of a stoppage of beating (quiescence) and a recovery of swimming in a straight path, followed by swimming in a circular path again; as the result the sperm avoided the obstacle. Ca^{2+} -imaging with Fluo-4 showed that the intracellular Ca^{2+} was high in the quiescence and gradually decreased after that. The effects of blockers and antibodies against candidate components revealed that the Ca^{2+} influx was induced by Ca^{2+} channels and the Ca^{2+} efflux was induced by a flagelliasialin-related Ca^{2+} -efflux system, plasma membrane Ca^{2+} -ATPases and the K^{+} -dependent $\text{Na}^{+}/\text{Ca}^{2+}$ exchanger. The results show that the Ca^{2+} -dependent mechanosensory behaviour of the sea urchin sperm is regulated by organized functioning of the membrane environment including the plasma membrane proteins and flagelliasialin.

Key words: avoiding response, calcium, flagelliasialin, plasma membrane Ca^{2+} -ATPase, K^{+} -dependent $\text{Na}^{+}/\text{Ca}^{2+}$ exchanger

Introduction

Ca^{2+} regulates various cellular activities. The flagellar movement of sea urchin sperm is one such activity. When demembranated sea urchin sperm flagella are reactivated by ATP, at low Ca^{2+} concentrations they alternately form in opposite directions slightly asymmetrical, propagating bends as in live sperm. The flagellar asymmetry is regulated by the intracellular Ca^{2+} concentration. Increasing the con-

centration of Ca^{2+} (10^{-7} – 10^{-5} M) increases the asymmetry (Brokaw *et al.*, 1974) and at 10^{-4} M the flagella are arrested with a cane-shape waveform (quiescence, Gibbons and Gibbons, 1980a). Wave asymmetry seems to be important for the regulation of swimming direction of the sperm of various organisms. Sperm of some sea urchins and those of the tunicate, *Ciona*, are known to show chemotactic responses to certain egg-related substances; that is, they sense the attracting factors released from the egg and change the asymmetry of flagellar waveforms (Kaupp *et al.*, 2003; Wood *et al.*, 2005; Shiba *et al.*, 2008). Chemotaxis, however, is not the sole response of swimming sperm that depends on Ca^{2+} -regulation of flagellar movement. Many kinds of ion channels and other membrane proteins related to Ca^{2+} transport in sperm membrane (Darszon *et al.*, 2006) may well be involved, through their organized functioning, in the Ca^{2+} -dependent regulation of flagellar movement in swimming behaviours of sperm.

The role of flagellar movements in sperm behaviour that depend on the intracellular Ca^{2+} has been studied under

*To whom correspondence should be addressed: Chikako Shingyoji, Department of Biological Sciences, Graduate School of Science, University of Tokyo, Hongo, Tokyo 113-0033, Japan.

Tel: +81-3-5841-4065, Fax: 81-3-5841-4385

E-mail: chikako@biol.s.u-tokyo.ac.jp

[†]Present address: Kogiku Shiba, Shimoda Marine Research Center, University of Tsukuba, Shizuoka 415-0025, Japan.

Abbreviations: MS, mechanical stimulation, mechanical stimulus (stimuli); polySia, polysialic acid; ASW, artificial sea water; suPMCA, sea urchin plasma membrane Ca^{2+} -ATPase; suNCKX, sea urchin K^{+} -dependent $\text{Na}^{+}/\text{Ca}^{2+}$ exchanger; CE, 5(6)-carboxyeosin; C_B, circular path before MS; Q, quiescence; S, straight path; C_A, circular path after MS.

several experimental conditions. When various kinds of stimulation such as a UV flash or electric stimulation is applied, live sea urchin sperm flagella stop beating with a principal bend at the base to assume a cane shape (Gibbons, 1980; Shingyoji and Takahashi, 1995). The response is induced by a depolarization of the flagellar membrane, which causes an influx of Ca^{2+} into the sperm flagellum through certain kinds of Ca^{2+} channels. It is interesting that similar responses are also induced by mechanical stimulation (MS) in other materials: in the gills of the mussel *Mytilus edulis*, MS induces a ciliary arrest response associated with a Ca^{2+} -dependent depolarizing receptor potentials (Murakami and Machemer, 1982). In the ciliate *Paramecium caudatum*, MS does not cause an arrest response but induces a temporary reversal in the beating direction of cilia to bring about backward swimming of the cell. This response is also dependent on the intracellular Ca^{2+} concentration (Naitoh and Kaneko, 1972). In the unicellular algae *Chlamydomonas reinhardtii*, mechanical agitation of the cell suspension is followed by Ca^{2+} -dependent activation of flagellar motility (Wakabayashi *et al.*, 2009). However, the effects of MS on the behaviour of sperm have not been well documented, although the effects on the movement of flagella themselves have been demonstrated (Okuno and Hiramoto, 1976; Shingyoji *et al.*, 1995; Ishikawa and Shingyoji, 2007).

In the present study, we developed a new experimental system to analyse behavioural responses of sperm to MS. MS of a sperm induced a characteristic series of waveform changes, consisting of a transient stoppage of beating (quiescence) with a cane-shape waveform, a straight swimming path with more symmetrical bending waves, and finally a resumption of the usual circular swimming path with more asymmetrical bending waves. By these sequential responses the sperm avoided the microstylus. Such “avoiding response” occurred only in the presence of a physiological concentration of Ca^{2+} in sea water. As the avoiding response is repeatable and stable, it enabled us to study the regulation of intracellular Ca^{2+} underlying the flagellar movement by using blockers and antibodies against candidate membrane proteins. We found that the avoiding response was inhibited not only by a stretch-activated ion channel blocker but also by an L-type voltage-dependent Ca^{2+} channel blocker. The antibody against flagelliasialin, a blocker of the plasma membrane Ca^{2+} -ATPases and a blocker of the K^{+} -dependent $\text{Na}^{+}/\text{Ca}^{2+}$ exchanger did not inhibit the response of the sperm to show quiescence, but inhibited the normal progression of response after the quiescence. Flagelliasialin (Miyata *et al.*, 2004, 2006), a sulfated $\alpha 2,9$ -linked polysialic acid (polySia)-bearing glycoprotein found exclusively on the sea urchin sperm membrane, may modulate a Ca^{2+} efflux system. Our results show that the Ca^{2+} -dependent mechanosensitivity plays a role in the swimming behaviour of the sperm, and the Ca^{2+} regulation in flagella is achieved by organized functioning of the membrane environment including Ca^{2+} transport proteins and flagelliasialin.

Materials and Methods

Sperm and solutions

Live sperm of the sea urchins, *Pseudocentrotus depressus* and *Hemicentrotus pulcherrimus*, were used throughout the study, except for the experiment of blockers and antibodies where those of *H. pulcherrimus* were mainly used. The sperm were suspended in 250,000 volumes of artificial sea water (ASW) containing 465 mM NaCl, 10 mM KCl, 10 mM CaCl_2 , 25 mM MgCl_2 , 28 mM MgSO_4 , 0.2 mM ethylenediaminetetraacetic acid (EDTA) and 5 (or 2) mM Tris-HCl (pH 8.0). Motility of the suspended sperm was evaluated and those which showed 80% or higher motility were used. For experiments at a lower Ca^{2+} concentration, we used 1 and 3 mM CaCl_2 . The low Ca^{2+} and low pH ASW (LASW) used for fluorescence imaging was the same as ASW except that its Ca^{2+} concentration was 1 mM and the pH was adjusted to 7.0.

The demembrated sperm used for Fig. 2Be were prepared as previously described (Shingyoji and Takahashi, 1995) and reacted at 0.5–1.0 mM ATP and 10^{-4} M Ca^{2+} .

Observation, recording and analysis

The suspended sperm was introduced into an observation chamber constructed with a slide glass and a coverslip with a one-side-opened silicone-rubber sheet of 1 mm thickness used as a spacer. The slide glass and the coverslip were coated with 0.05% (w/v) formvar or 1% BSA to avoid attachment of sperm to the glass surface.

Flagellar movements of the swimming sperm were observed at room temperature (20–25°C) under a phase contrast microscope (Olympus BX51) with a $\times 20$ objective (Olympus UPlan FINH). The stroboscopic lighting system with a power LED was used as previously described (Shiba *et al.*, 2006). Individual images of the sperm flagella were recorded on a personal computer (PC) by using a capture card (HAS-PCI, Ditect, Tokyo, Japan) connected to a high-speed CCD camera (HAS-200, Ditect, Tokyo, Japan) at a rate of 200 frames/sec. The position of each sperm head and the flagellar waveform were tracked automatically and the sperm head trajectories, swimming path curvature, flagellar curvature and shear angle were calculated by using the cell motility analysis software, Bohboh (Bohboh Soft, Tokyo, Japan (Shiba *et al.*, 2002)). Flagellar asymmetry was quantified as the ratio of the maximal curvature of the principal bend to that of the reverse bend ($\text{P-bend}_{\text{Max}}/\text{R-bend}_{\text{Max}}$), according to the definition by Gibbons and Gibbons (1972). The method to determine the curvature was based on Baba and Mogami (1985). We refer to this ratio to evaluate the degree of flagellar asymmetry.

Flagellar movements of head-attached sperm were observed under a Zeiss Axiovert 35 with phase-contrast optics and recorded with a high-speed video system (MHS 200, nac Image Technology Inc., Japan) at 200 fps. Xenon strobe flashes (Model 271C, Chadwick-Helmuth Co. Inc., USA) were used for illumination. Observation of the effects of blockers and antibodies on the avoiding responses of sperm induced by MS was carried out on an

inverted microscope (Nikon TMD) with a dark-field optics and using a CCD camera (Neptune 100, Watec, Japan) with an image intensifier (DII-2050CH, Nakanishi Image Lab. Inc., Japan) and a VHS video cassette recorder (HR-B12, Victor, Japan) for recording under a stroboscopic illumination.

Mechanical stimulation

A glass microstylus with a tip diameter of 0.1 μm or less was made from a thin glass rod (1 mm in diameter) by using a needle puller (Narishige PN-3, 8508). The microstylus was attached to a water-pressure micromanipulator (Narishige, MO-103) attached to the microscope. For the experiments using freely swimming sperm (Fig. 1, Fig. 3 and Fig. 4), the microstylus was placed in the trajectory of a swimming sperm in ASW so that the sperm head collided vertically with this microstylus under the microscope. For the second experiment using head attached sperm (Fig. 2), the microstylus was moved at a velocity of 2–500 $\mu\text{m}/\text{sec}$ with an amplitude of 1–2 μm by a piezo-electric device, triggered with a linear ramp (for 2–500 $\mu\text{m}/\text{sec}$) and with a square pulse of 1–1.5 sec duration (for 100–500 $\mu\text{m}/\text{sec}$). There were no large differences between the data obtained by the two trigger procedures.

Fluorescence imaging of swimming sperm flagella

Dry sperm was suspended in 4–5 volumes of LASW containing 0.05% wt/vol cremophorEL and 20 μM Fluo-4 AM and incubated with rotation for 2 h at 20°C. Fluo-4 AM was from Molecular Probes (Eugene, OR, USA) and cremophorEL was from Nacalai Tesque (Kyoto, Japan). The loaded sperm was diluted 10^4 to 10^5 -fold in ASW. The sperm suspension was immediately placed into the observation chamber constructed as described above except that it was made from two coverslips without using a glass slide. Fluorescence signals from swimming sperm were captured at room temperature (20–25°C) through an inverted microscope (Olympus IX71) with a $\times 60$ objective (Olympus PlanApo) using an Olympus filter set (excitation filter, BP490–500; dichromatic mirror, DM505; emission filter, BA510–550) and recorded on a PC connected to a digital CCD camera (Retiga Exi, QImaging, Burnaby, Canada) at 50 fps using the imaging application (TI workbench). For fluorescence illumination the stroboscopic lighting system with a power LED was used as previously described (Shiba *et al.*, 2008). The intensity of the fluorescence signals and sperm mechanosensory behavior were also analysed by Bohboh software. $[\text{Ca}^{2+}]_i$ was expressed as F/F_0 , where F is the fluorescence signal intensity of the flagellum averaged along its entire length and F_0 is the minimum value of the signal intensity observed for each response.

Blockers of membrane proteins

Gadolinium chloride and cobalt chloride were obtained from Wako (Osaka, Japan). Verapamil hydrochloride, pimozide and 5(6)-carboxyeosin (CE) were obtained from Sigma-Aldrich (St. Louis, MO, USA). KB-R7943 mesylate was obtained from Tocris (Ellisville, MO, USA). Gadolinium, cobalt and verapamil were

dissolved in water, and pimozide, CE and KB-R7943 were dissolved in dimethyl sulfoxide. When the sperm were suspended in ASW for observation of their swimming, each blocker was added to ASW to obtain final concentrations as follows: 10–40 μM Gd^{3+} , 3 mM Co^{2+} , 0.1 mM verapamil, 10 μM pimozide, 1–3 μM CE and 1–2 μM KB-R7943 (Wakabayashi *et al.*, 2009; Gunaratne *et al.*, 2006; Su and Vacquier, 2002). For the experiments of Gd^{3+} , we used ASW without EDTA. Observation under a microscope started immediately after the addition of the blockers. All experiments were carried out at room temperature (22–26°C).

Antibodies against flagelliasialin

A hybridoma cell 4F7 that produces monoclonal IgG specific for $\alpha 2,9$ -linked polysialic acid (polySia) structure (Miyata *et al.*, 2006) and a hybridoma cell 3G9 that produces monoclonal IgM specific for 8-*O*-sulfated sialic acid residue (Ohta *et al.*, 1999; Yamakawa *et al.*, 2007) were established and grown in serum-free medium (CosMedium001, Cosmobio, Tokyo, Japan). Monoclonal antibodies 4F7 and 3G9 were purified from culture supernatants by precipitation with 50% saturated ammonium sulfate, followed by gel filtration chromatography on Sephacryl S-300 (GE Healthcare). These two antibodies recognize the carbohydrate part of flagelliasialin, because it consists of an $\alpha 2,9$ -polySia chain capped by an 8-*O*-sulfated sialic acid residue (Miyata *et al.*, 2004). To inhibit the flagelliasialin function, we used mAb 4F7, which specifically recognizes flagelliasialin, because the $\alpha 2,9$ -linked polySia structure only exists in flagelliasialin in sea urchin sperm (Miyata *et al.*, 2006), and we used mAb 3G9 as a control.

Results

Mechanosensory behavioural responses of the sea urchin sperm

The sperm of the sea urchins, *P. depressus* and *H. pulcherrimus*, suspended in artificial sea water containing 10 mM Ca^{2+} swim close to the formvar-coated glass surface in circular paths with a diameter of about 50 μm at a speed of 130–250 $\mu\text{m}/\text{sec}$ (Fig. 1A, upper panels; Fig. 1C, blue). When a glass microstylus was placed in the swimming trajectory of a sperm and the sperm head collided vertically with the microstylus, the sperm showed a transient stoppage of beating (quiescence) for about one second (we call this period the arrest phase or quiescence), after which it resumed beating, this time showing a more straight swimming path than before the stimulation (the straight path phase) (Fig. 1C, S in the left diagram and the decrease of path curvature after 2 sec). As a result the sperm avoided the obstacle (Fig. 1A, lower panels; Fig. 1C, red). The speed of collision was about 100–200 $\mu\text{m}/\text{sec}$ and the average duration of the arrest phase was 1.52 ± 1.38 sec (mean \pm s.d., $n=36$; the range was 0.14–8.12 sec). In most cases, the collision made the swimming path turn backward by about

100–240 degrees from the original swimming direction (the turning angle was measured as θ shown in Fig. 1C). After the straight swimming phase of a few seconds, the sperm resumed their original beating to swim in a circular path. This series of flagellar responses to MS was also observed in at least three more species of sea urchins, *Anthocardaris crassispina*, *Strongylocentrotus nudus* and *Strongylocentrotus intermedius*, indicating that this avoid-

ing response of sperm is ubiquitous in sea urchins.

The avoiding response consisting of the above described series of behavioural changes, that is, a circular path before MS (C_B) → quiescence (Q) → a straight path (S) → a circular path after MS (C_A), was observed in 100% of the sperm in the presence of 10 mM Ca^{2+} ($n=57$) (Fig. 1A and C), but in 14.5% and 5.4% of them in the presence of 3 mM Ca^{2+} ($n=55$) (Fig. 1B, left panels) and 1 mM Ca^{2+} ($n=37$), respectively. No such avoiding response was observed in the absence of Ca^{2+} but the trajectory of circular paths of the sperm moved slightly from the position before the stimulation (Fig. 1B, right panels). In the presence of 1 mM Ca^{2+} , most of the mechanically stimulated sperm did not show a stoppage of beating but their circular paths shifted slightly (Fig. 1B, middle panels; Fig. 1D, left) without a change in the path curvature (Fig. 1D, right), in a similar manner to that observed in the absence of Ca^{2+} . The curvature of a swimming trajectory (we call this the swimming path curvature) can be defined as a reciprocal of the radius of the circular swimming path obtained from the trajectory of the head. Fig. 1E and F show changes of the average curvature of the swimming path during C_B (blue) and S – C_A (red) at 10 mM Ca^{2+} and 1 mM Ca^{2+} , respectively. The average path curvature just at 0–1 sec in the presence of 10 mM Ca^{2+} is very small (0.012 – $0.024 \mu\text{m}^{-1}$) which means that the swimming path just after the quiescence is very close to a straight line in the S phase.

To obtain further information about the mechanosensitivity of the sperm head, we applied mechanical stimuli (MS) with a glass microstylus to sperm that were attached by the side of their heads to the surface of a formvar-coated

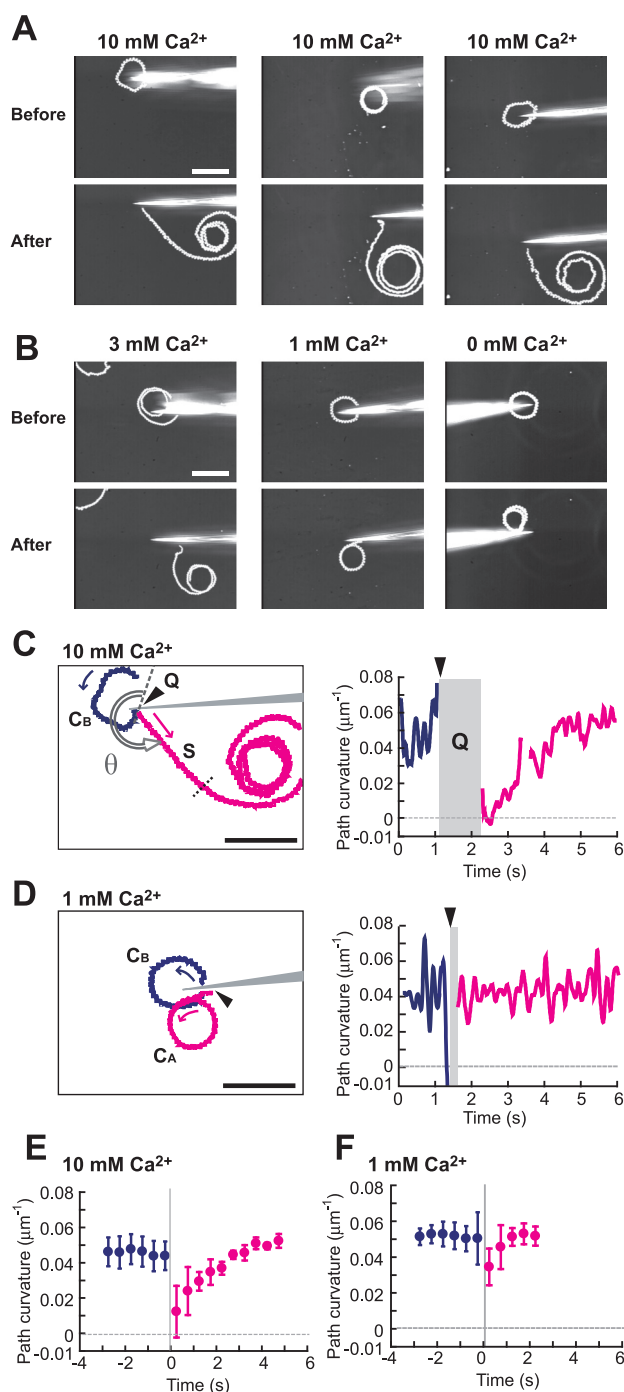


Fig. 1. Responses of swimming sperm to mechanical stimulation (MS) in the presence of 10 mM (A, C, E) and 0–3 mM (B, D, F) Ca^{2+} in ASW. (A, B) Video images showing swimming trajectories of sperm heads before (upper panels) and after (lower panels) MS. Before MS the sperm swam in circular swimming paths (white circles). A glass microstylus (white rods) was inserted from the right side of the panel except in the images taken at 0 mM Ca^{2+} , in which it was inserted from the left side, and its tip was placed into the circular path. After the collision of the sperm head with the microstylus at 10 mM Ca^{2+} , the sperm trajectory changed to a straight path for a while and then resumed a circular path (A). In the presence of 3 mM Ca^{2+} , a similar avoiding response was observed (B, left). In contrast, in the presence of 1 mM Ca^{2+} and in the absence of Ca^{2+} (B, middle and right), most sperm swam in circles after the MS. Bars, 50 μm . (C, D) Changes in the curvature of the trajectory (path curvature) of a sperm swimming in the presence of 10 mM (C) and 1 mM (D) Ca^{2+} in ASW. The same responses as those shown in the left panels of A and in the middle panels of B are used for C and D, respectively. Blue and red lines indicate before and after the MS, respectively. The timing of the collision of sperm heads with the microstylus is indicated by arrowheads. The turning angle of the swimming sperm at the MS is indicated by θ in C. C_B , Q, S and C_A indicate the four phases of sperm movement. Grey boxes indicate the period of quiescence (Q in C) or sequential changes of bending waves (D) caused by the collision. Changes of the average swimming path curvatures (mean \pm s.d.) at 10 mM ($n=36$) and 1 mM ($n=6$) Ca^{2+} are shown in E and F, respectively. In these graphs the periods of the arrest phase are omitted.

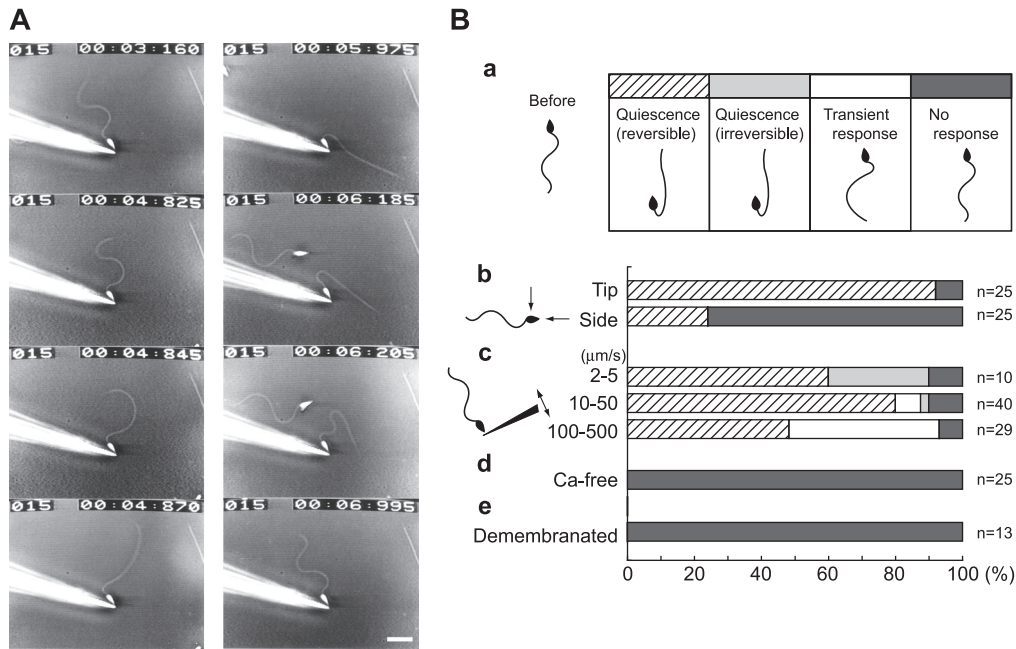


Fig. 2. Responses induced by MS of sperm attached by their heads to the glass surface in the presence of 10 mM Ca^{2+} in ASW. The microstylus (from the left) was manipulated by a piezo-electric device. Sequential video images (A) show normal beating before MS (left top panel), MS by collision of the microstylus (from 04:825 (4 sec and 825 ms) to 05:975), and recovery of beating after the MS (right, the last three panels). Responses to the MS are categorized into four patterns (Ba): quiescence followed by recovery of beating (hatched box), quiescence without recovery (grey box), transient waveform changes (open box), and no response (filled box). The frequency of occurrence of these patterns changed depending on the region of MS in the sperm heads (Bb), but the speed of MS applied to the tip of the sperm head (Bc) did not have a large effect. In the absence of Ca^{2+} in ASW (Bd) and in demembrated sperm (Be) mechanosensory behaviour of the sperm was not induced. The speed of MS in Bb, d and e was 10–50 $\mu\text{m}/\text{sec}$.

glass slide and whose flagella were beating regularly. Sequential video images of the experiment are shown in Fig. 2A, where the microstylus (from the left) manipulated by a piezo-electric device collided with the tip of the sperm head between the panels 04:825 (4 sec and 825 msec) and 05:975, during which the flagellum stopped beating and became quiescent. After the collision the sperm resumed beating. The flagellar responses to such MS fell into four types (Fig. 2Ba): the reversible quiescence type (hatched box) is a response similar to that shown in Fig. 2A; the irreversible quiescence type (grey box), in which the sperm did not resume swimming after the quiescence; the transient response type (open box), in which the stoppage of beating occurred without assuming a quiescent form; and a fourth type, in which there was no response (filled box). The distribution of the four types showed local differences in mechanosensitivity, that is, the anterior end of the head was more sensitive to MS. The increase of the reversible quiescence type in the MS applied to the tip of head compared to that in MS applied to the side of the head was statistically significant (Fig. 2Bb; $p < 0.001$, Fisher's exact test). However, the wide differences in the velocity of collision had only a small effect on the induction of reversible responses (Fig. 2Bc). In this experiment, Ca^{2+} and the presence of the membrane were also indispensable (Fig. 2B, d and e).

Imaging of the Ca^{2+} dynamics

Wave asymmetry seems to play an important role in the regulation of swimming direction of many sperm and has been thought to be regulated by the intracellular Ca^{2+} concentration (Brokaw, 1979; Gibbons and Gibbons, 1980a). To understand the relationship between the dynamics of Ca^{2+} and the control of swimming direction in beating flagella, analysis of the sperm showing the avoiding response seems particularly useful, because the response involves all the essential patterns of flagellar movements that determine the swimming direction of spermatozoa. Using swimming sperm loaded with Fluo-4, we carried out real-time imaging of the flagellar waveforms and the intracellular Ca^{2+} before and after the collision of their heads with the glass microstylus (see Supplementary Movie 1) in a similar setup as shown in Fig. 1. During the stable circular swimming before the MS, the sperm showed a low, stable fluorescence signal of Ca^{2+} (Fig. 3A–D, panel 1 and point 1; Fig. 3C, C_B). We found that the intracellular concentration of Ca^{2+} increased transiently when the sperm collided with the microstylus (Fig. 3A–D, panel 3 and point 3), which was associated with the quiescence of the sperm. The Ca^{2+} concentration gradually decreased but was still maintained at a high level during the arrest phase (Fig. 3A–D, panels 3 and 4, and changes

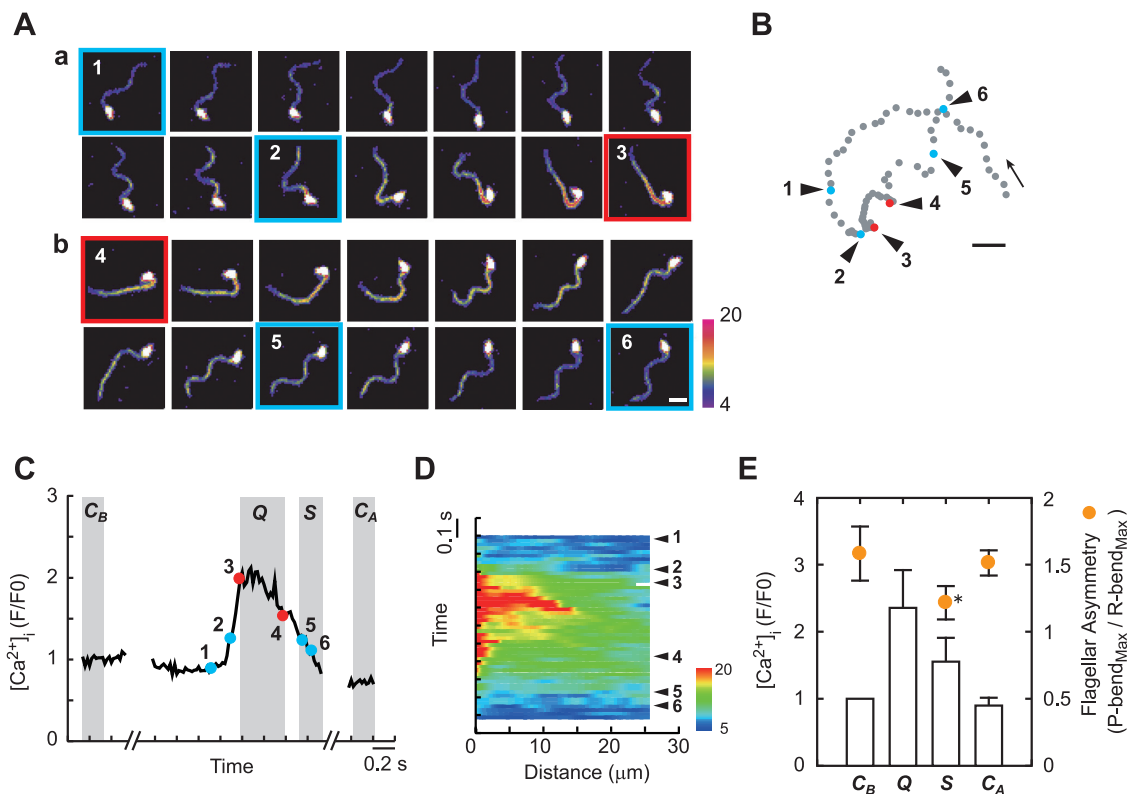


Fig. 3. Changes in the intracellular Ca^{2+} concentration in the avoiding response observed in the same sperm (A–E). A, Sequential fluorescence images of *P. depressus* sperm taken at 20 ms intervals before (a), and immediately after (b), the quiescence (panels 3 and 4) induced by MS. The sperm collided with the microstylus between panels 2 and 3. The colour scale (from 4 to 20) is the look-up table (LUT) for the intensity of fluorescence signal. Bar, 10 μm . The numbered arrowheads (B and D) and points (C) correspond to the numbered images shown in A. B, Trajectory of the sperm head. The direction of swimming is indicated by an arrow. Bars, 10 μm . C, Changes in the normalized concentration of intracellular Ca^{2+} (F/F_0). F is the fluorescence signal intensity of the flagellum averaged along its entire length. F_0 is the minimum value of the signal intensity obtained in this series of response. D, Changes with time of the fluorescence signal shown against the distance along the flagellum from its base (1 μm division). E, Intracellular concentration of Ca^{2+} (F/F_0) and flagellar asymmetry. Average values (mean \pm s.d.) of intracellular Ca^{2+} (F/F_0) (open boxes) and flagellar asymmetry (points with error bars) during the circular path phase before MS (C_B), quiescence (Q), straight path phase (S) which was measured as a steady-state beating phase for 0.2 sec after the Q and the circular path phase after MS (C_A) were obtained from the images recorded during each phase shown as four grey-bands in C. The numbers of the image used for measurement were 13(C_B), 11(Q), 15(S) and 5(C_A). Flagellar asymmetry in phase S, indicated with an asterisk, was significantly lower than that in phase C_B ($P < 10^{-4}$, Student's t-test).

between points 3 and 4). The arrest phase consisted of quiescence and in some cases transient twitch-like movements (Gibbons and Gibbons, 1980b) consisting of formation and relaxation of bends localized at the base of the flagellum, alternating with quiescence. In this example of Fig. 3A, only the first and the final quiescence states (3 and 4) in the arrest phase are shown. More precise observation showed a large increase in the Ca^{2+} concentration in the basal region of the flagellum in the first quiescence state (Fig. 3D, point 3), indicating that the Ca^{2+} influx occurred in this region and spread toward the tip (0.1–0.2 sec after point 3) during the arrest phase. After the arrest phase the Ca^{2+} concentration continued to decrease but was still at a higher than normal level during the straight path phase (Fig. 3A–D, panels 5 and 6, and changes between the points 5 and 6). When the sperm resumed swimming in a circular path the concentration of

Ca^{2+} decreased to a low level (Fig. 3C, in C_A) similar to that before the collision (Fig. 3C, in C_B).

As shown in Fig. 3E, the above described changes of Ca^{2+} dynamics were characteristic of each phase: the intracellular Ca^{2+} concentration is low during the circular path both before (C_B) and after (C_A) the MS, it is at a highest level in the quiescent or arrest phase (Q) and at a medium level during the straight path phase (S). Analysis of the degree of asymmetry of the flagellar waveforms (Fig. 3E, yellow circles) showed more symmetrical bending waves for the straight path (Fig. 3E, during S) than for the circular path (Fig. 3E, during C_B and C_A). The difference between C_B and S was significant but that between C_B and C_A was not. This indicates that the symmetrical beating phase occurs at a higher than normal concentration of Ca^{2+} . The wave symmetry during the straight path appeared to be caused by an

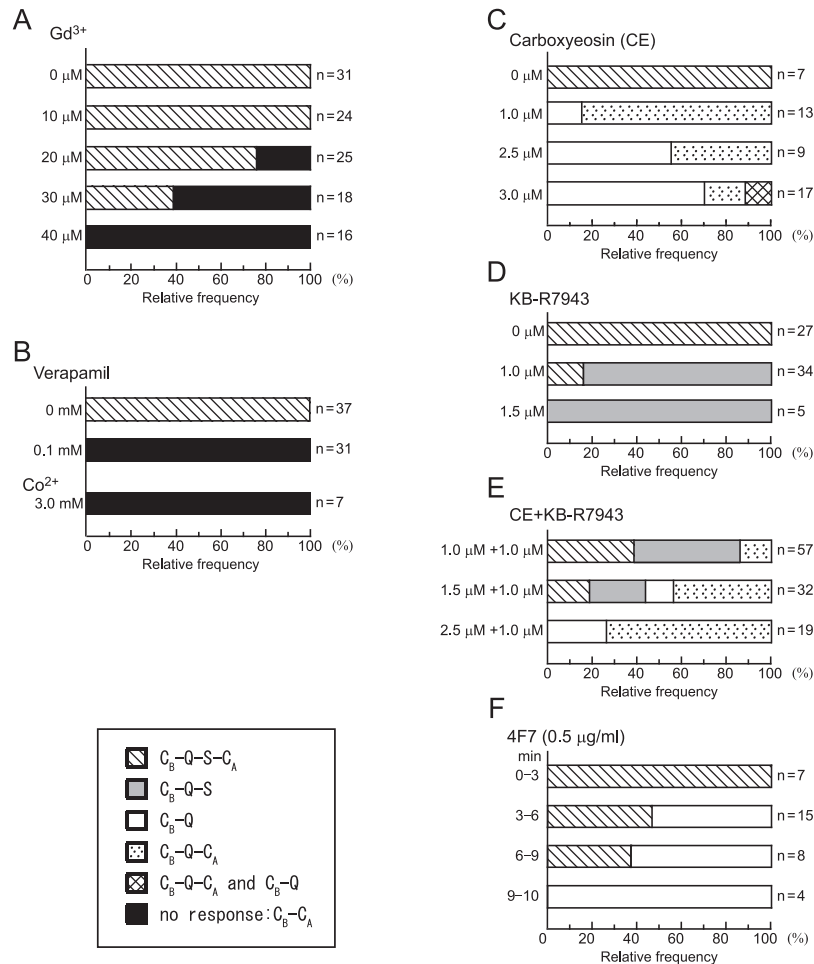


Fig. 4. Effects of various blockers and an antibody on the avoiding response induced by MS. Without blockers, the MS induced in all sperm the $C_B-Q-S-C_A$ series of responses (hatched boxes) in ASW. In the presence of 10–30 and 40 μM Gd^{3+} , a blocker of stretch-activated ion channels, the avoiding response was partly and completely inhibited, respectively, and the sperm that swam in a circular path before and after the MS (A, filled box, C_B-C_A type response) appeared. The avoiding response was also inhibited by 0.1 mM verapamil, an L-type voltage-dependent Ca^{2+} channel blocker, and by 3 mM Co^{2+} (B). In the presence of 5(6)-carboxyeosin (CE) the normal avoiding response did not occur but the sperm showed a sequential avoiding response without the straight path phase (C, dotted boxes, C_B-Q-C_A type response), or became immotile with a quiescent waveform (C, open boxes, C_B-Q type response). The C_B-Q type responses increased with the concentration of carboxyeosin. A part of the sperm that showed the C_B-Q-C_A type response showed the C_B-Q type response on the second MS (C, cross-hatched box). The presence of 1 and 1.5 μM KB-R7943, a blocker of Na^+/Ca^{2+} exchanger, inhibited the normal progression of response after the straight path phase (D, grey box, C_B-Q-S type response). In the presence of 1–2.5 μM CE with 1 μM KB-R7943, combinations of the four types of response, $C_B-Q-S-C_A$, C_B-Q-S , C_B-Q and C_B-Q-C_A , were observed (E). 4F7, a monoclonal antibody against the $\alpha 2,9$ -linked polysialic acid structure of flagelliasialin, inhibited the normal progression of response after the arrest phase (F, open boxes, C_B-Q type response). The occurrence of this response increased with the treatment time up to 10 min.

increase in the curvature of the reverse bends without an appreciable change in the principal bends (data not shown).

Regulation of Ca^{2+} entry

To elucidate the mechanism regulating the Ca^{2+} dynamics in the flagellar responses to MS, the effects of several blockers and antibodies on the avoiding response were studied. We found that the avoiding response was inhibited by a stretch-activated ion channel blocker Gd^{3+} (Yang and

Sachs, 1989; Yoshimura, 1996; Krasznai *et al.*, 2003; Wakabayashi *et al.*, 2009). In the presence of 10 μM Gd^{3+} , MS always induced the avoiding response of the swimming sperm ($n=24$). However, 20 and 30 μM Gd^{3+} partly inhibited the avoiding response, and at 40 μM Gd^{3+} the avoiding response was completely inhibited and all the sperm that collided with the microstylus continued to swim ($n=16$) (Fig. 4A) as those swimming in the absence of Ca^{2+} . An L-type voltage-dependent Ca^{2+} channel blocker verapamil (0.1 mM) (Wakabayashi *et al.*, 2009), as well as 3 mM

Co^{2+} (Shingyoji and Takahashi, 1995), also inhibited the avoiding response (Fig. 4B). In the presence of these Ca^{2+} channel blockers, the sperm continued to swim in a circular path even after the collision with the microstylus. However, a T-type Ca^{2+} channel blocker pimoziide (10 μM) did not inhibit the mechanosensory behaviour of the sperm ($n=12$). These results show that the influx of Ca^{2+} that induces the quiescence as the first step in the avoiding response is regulated by the combination of stretch-activated ion channels and L-type voltage-dependent Ca^{2+} channels.

Roles of Ca^{2+} -ATPases and K^{+} -dependent $\text{Na}^{+}/\text{Ca}^{2+}$ exchanger

In the avoiding response, the arrest phase is followed by a decrease in the intracellular Ca^{2+} concentrations. The plasma membrane proteins contributing to Ca^{2+} efflux that have been demonstrated in sea urchin sperm are the plasma membrane Ca^{2+} -ATPases (suPMCA) and the K^{+} -dependent $\text{Na}^{+}/\text{Ca}^{2+}$ exchanger (suNCKX) (Su and Vacquier, 2002; Gunaratne *et al.*, 2006). We examined the effects of a blocker of the suPMCA, 5(6)-carboxyeosin (CE) (Gunaratne *et al.*, 2006), and a blocker of the suNCKX, KB-R7943 (Su and Vacquier, 2002; Shiba *et al.*, 2006; Rodríguez and Darszon, 2003), on the avoiding response. It has been reported that the motility of the swimming sperm is largely inhibited by CE at 5 μM (Gunaratne *et al.*, 2006). We found that even at 1 μM CE, MS did not induce the normal $\text{C}_\text{B-Q-S-C}_\text{A}$ series of avoiding response (Fig. 4C). Instead, it induced new type of sequential responses, i.e. $\text{C}_\text{B-Q-C}_\text{A}$. Similar responses were observed during 5–10 min of treatment with CE. Increasing the concentration of CE, however, decreased the proportion of the $\text{C}_\text{B-Q-C}_\text{A}$ type response and increased the proportion of the $\text{C}_\text{B-Q}$ type response, in which the sperm remained immotile after the quiescence induced by the MS. These changes with the CE concentration (1–3 μM) were statistically significant (Fig. 4C; $p<0.01$, Fisher's exact test). In the presence of 3 μM CE, 70% of the sperm ($n=17$) showed the $\text{C}_\text{B-Q}$ type response to the first MS (Fig. 4C, open box), while among the five sperm that showed a $\text{C}_\text{B-Q-C}_\text{A}$ type response to the first MS, two sperm and three sperm respectively showed the $\text{C}_\text{B-Q}$ type response (Fig. 4C, cross-striped box) and the $\text{C}_\text{B-Q-C}_\text{A}$ type response (Fig. 4C, dotted box) to the second stimulus. Such changes of the response types, from $\text{C}_\text{B-Q-C}_\text{A}$ to $\text{C}_\text{B-Q}$, were not observed at lower concentrations of CE. After a 10 min treatment with 3 μM CE, the sperm gradually stopped swimming and most of the immotile sperm showed quiescent waveforms.

The blocker of suNCKX, KB-R7943, did not inhibit the response of the sperm in the arrest phase but inhibited the normal progression of response after the straight path phase (Fig. 4D). As a result, MS in the presence of the blocker (1–1.5 μM) induced the $\text{C}_\text{B-Q-S}$ type responses. In such responses, the straight path became longer than several 100

μm and in most cases the swimming path went away from the vicinity of the glass surface, making it difficult to follow the whole length of the path. Nevertheless, in two cases at 1 μM we could chase the sperm until the end of the straight path phase and found that they became immotile with a straight flagellum. This is consistent with the observation that more than 10 min of treatment with the blocker gradually decreased the proportion of sperm swimming in a circular path, as more symmetrical waves reduced the swimming path curvature, and finally the sperm became immotile with a straight flagellum. The results suggest that the suNCKX is responsible for decreasing the Ca^{2+} concentration in the final step of the avoiding response, from the straight path phase to the circular path phase.

Finally, to gain more insight into the regulation of suPMCA and suNCKX activities we examined the effects of the presence of both KB-R7943 and CE on the MS-induced avoiding response. When 1 μM KB-R7943 was present in addition to 1–2.5 μM CE, the mechanically-stimulated sperm showed four types of response: the $\text{C}_\text{B-Q-S-C}_\text{A}$, $\text{C}_\text{B-Q-S}$, $\text{C}_\text{B-Q}$ and $\text{C}_\text{B-Q-C}_\text{A}$ type responses (Fig. 4E), which are of the same types as those observed in the presence of CE (Fig. 4C) and of KB-R7943 (Fig. 4D). The presence of these two kinds of blockers induced cumulative effects of each blocker. It is interesting that the $\text{C}_\text{B-Q-S-C}_\text{A}$ type response, which did not appear in the presence of CE alone, was observed at a higher proportion in the presence of 1 μM CE with 1 μM KB-R7943 than in the presence of 1 μM KB-R7943 alone (Fig. 4C, D and E). This feature did not appear in the presence of 2.5 μM CE with 1 μM KB-R7943, whereas the proportion of $\text{C}_\text{B-Q-C}_\text{A}$ type response increased compared to that in the presence of CE alone. Furthermore, the $\text{C}_\text{B-Q}$ type response, which would be expected to appear when the intracellular Ca^{2+} concentration is elevated by the presence of the two kinds of blockers, was induced but at a lower proportion than in the presence of CE alone. These results suggest that the activities of suPMCA and suNCKX are not regulated solely by the intracellular Ca^{2+} concentration but are also controlled by their mutual interaction.

Roles of flagelliasialin

To clarify the role of flagelliasialin, we used monoclonal antibodies against the $\alpha 2,9$ -linked polySia structure (4F7) and 8-*O*-sulfated sialic acid residue (3G9); the former specifically recognizes flagelliasialin and inhibits the swimming of sea urchin sperm at 1 $\mu\text{g}/\text{ml}$ (Miyata *et al.*, 2006). We found that 4F7 (0.5 $\mu\text{g}/\text{ml}$) did not inhibit the response of the sperm in the arrest phase but inhibited the normal progression of response after the arrest phase induced by MS, and that the sperm did not resume beating after the quiescence. 3G9 (1–2 $\mu\text{g}/\text{ml}$) did not inhibit the series of avoiding response to MS ($n=17$). The $\text{C}_\text{B-Q}$ type responses were induced by the MS after 3 min of treatment with 4F7 and

their frequency of occurrence increased with the increase of treatment time up to 10 min (Fig. 4F). The increase was statistically significant (Fig. 4F; $p < 0.01$, Fisher's exact test). Induction of the C_B -Q type response is very similar to the effects of CE, except that 4F7 did not induce the C_B -Q- C_A type response but induced the normal C_B -Q-S- C_A type response at its lower concentrations. In the case of CE, the responses induced by the MS were little affected by the treatment within 10 min, after which the number of immotile sperm showing a quiescent waveform increased. In contrast, the effects of 4F7 depended on the treatment time and the numbers of immotile sperm showing quiescence or a quiescence-like waveform with a smaller bend increased with time after 5 min of treatment. To examine the effect of pretreatment with 4F7 on the immotile sperm in the presence of Ca^{2+} and on the motile sperm in the absence of Ca^{2+} , the sperm were treated with 4F7 for 5 min at low pH (6.8–7.0) and 10 mM Ca^{2+} and for 10 min at 0 mM Ca^{2+} and pH 8.0, respectively, and then diluted with 500 volumes of ASW at pH 8.0 and 10 mM Ca^{2+} containing 4F7. This pretreatment did not shorten the time necessary for inhibition of the sperm motility in ASW at pH 8.0 and 10 mM Ca^{2+} , indicating that the swimming-dependent reaction in the presence of Ca^{2+} is needed to induce motility inhibition.

Continuous beating in the presence of blockers

After a 10 min treatment with 4F7, most sperm became immotile with quiescence or quiescence-like waveform, which was very similar to the effect of CE. KB-R7943 also induced immotility but with a straight flagellum. Furthermore, regardless of the kinds of blockers, 5–10 min was the critical length of treatment to observe the drug-specific responses to MS. If these arrest responses with the blockers-specific waveforms are related to a gradual increase of the intracellular Ca^{2+} concentration, there may be Ca^{2+} entry through the Ca^{2+} channels. We tested the effect of verapamil and Co^{2+} on the inhibition of beating by 4F7, KB-R7943, and CE. In the presence of 0.1 mM verapamil (or 3 mM Co^{2+}) and 0.5 μ g/ml 4F7 all sperm continued stable swimming over 20 min. Similar stable swimming was observed in the presence of KB-R7943 with verapamil, and CE with verapamil. Ca^{2+} -imaging with Fluo-4 in the presence of 4F7 and Co^{2+} showed that the fluorescence intensity of intracellular Ca^{2+} concentration in the flagellum was about 70% (data not shown) of that of sperm swimming in circular paths in ASW (Fig. 3C, C_B and C_A). These observations indicate that in sea urchin sperm the intracellular Ca^{2+} concentration is maintained at a low level during swimming by balancing the Ca^{2+} influx, probably through the verapamil (or Co^{2+})-sensitive Ca^{2+} channels, with the Ca^{2+} efflux through the flagellarialin-related system, the suPMCA and the suNCKX.

Discussion

Mechanosensory responses of sperm

The present study has shown that sea urchin sperm respond to MS applied to the tip of their head by changing flagellar waveforms, thereby enabling the sperm to avoid the obstacle. The mechanosensory response requires Ca^{2+} in the medium (ASW) and progresses as a series of four characteristic behavioural phases in the swimming path curvature: circular path phase before MS (C_B) → quiescence or arrest phase (Q) → straight path phase (S) → circular path phase after MS (C_A). Such C_B -Q-S- C_A type responses were always induced in the sperm that responded to MS in the presence of 10 mM Ca^{2+} . We have found that throughout the C_B -Q-S- C_A type response, the intracellular Ca^{2+} concentration in flagella is systematically regulated by Ca^{2+} transport proteins. Fig. 5 shows the outline of the present results. The changes in Ca^{2+} concentration throughout the typical response are estimated as follows: 10^{-8} M (during C_B) → 10^{-4} M (during Q) → gradual decrease $\sim 10^{-6}$ M (during S) → 10^{-8} M (during C_A). The Ca^{2+} concentration at S phase is simply inferred from the concentration for quiescence (Gibbons and Gibbons, 1980a) and that for normal swimming of the circular path phase (Brokaw, 1991) as their intermediate.

The mechanosensory response of the sea urchin sperm observed in this study is similar to that of *Paramecium*, in which mechanical stimuli are received at the anterior end of the cell body and cause changes in Ca^{2+} in the cilia (Ogura and Takahashi, 1976; Ogura and Machemer, 1980), whereas it differs from that in *Chlamydomonas*, which responds to MS applied to their flagella (Yoshimura, 1996; Wakabayashi *et al.*, 2009). In spite of the difference in the site of mechanoreception between sperm and *Chlamydomonas*, however, the inhibitory effects of Gd^{3+} and verapamil on the MS-induced responses similar to those demonstrated in *Chlamydomonas* (Yoshimura, 1996; Wakabayashi *et al.*, 2009) have been observed in sea urchin sperm. As voltage-dependent Ca^{2+} channels are found in the head and flagellum of sea urchin sperm (Darszon *et al.*, 2006), our results of the Ca^{2+} imaging (Fig. 3D) indicate that the first step in the MS-induced response involves cooperative activation of stretch-activated ion channels and the voltage-dependent Ca^{2+} channels in the sperm head, which subsequently would activate the voltage-dependent Ca^{2+} channels in the flagellum. The present observation that a large increase of Ca^{2+} occurs in the basal region of the flagellum during quiescence (Fig. 3D) indicates that the head-flagellum region is the predominant site of Ca^{2+} entry to induce quiescence. Ca^{2+} stores, thought to exist in the sperm head may also be related to the regulation of Ca^{2+} entry (Darszon *et al.*, 2001, 2006).

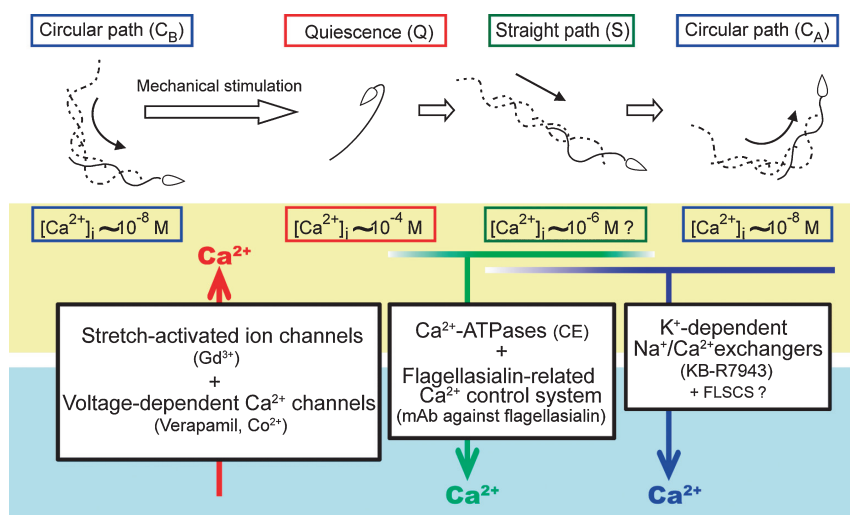


Fig. 5. Schematic diagram showing a model of the mechanism regulating the Ca^{2+} -dependent mechanosensory response in sea urchin sperm. Upper panels show a series of MS-induced changes in the behaviour of a sperm, consisting of the usual circular path with asymmetrical bending waves before MS (C_B), stoppage of beating (quiescence) with a cane-shape waveform (Q), a straight path with more symmetrical bending waves than those of C_B (S), and a circular path after MS with more asymmetrical bending waves (C_A) in the presence of 10 mM Ca^{2+} in ASW. Lower panels are our interpretation of the results, indicating changes of the intracellular Ca^{2+} concentration (yellow) during the course of the mechanosensory response and the membrane components (white boxes) involved in the regulation of Ca^{2+} dynamics. Chemicals shown in parentheses in the white boxes are those used to identify the membrane components. MS triggered the Ca^{2+} -entry (red arrow) from outside (blue) to inside (yellow) the sperm by coordinated activation of stretch-activated ion channels and voltage-dependent Ca^{2+} channels. Ca^{2+} -efflux occurred at two steps: the plasma membrane Ca^{2+} -ATPases and a flagelliasialin-related Ca^{2+} -control system (FLSCS) contribute to the first step from Q to S (green arrow), while the second step from S to C_A (blue arrow) requires a K^+ -dependent Na^+/Ca^{2+} exchanger. FLSCS might also be involved in the regulation of K^+ -dependent Na^+/Ca^{2+} exchanger.

Control of swimming direction and Ca^{2+} dynamics

In the avoiding response, swimming organisms control the direction of their movement. Moving directly backwards, with the rear (posterior) end of the organism leading, is an effective way to avoid the obstacle, which is observed in *Paramecium* (Naitoh and Kaneko, 1972). In sea urchin sperm, however, collision with an obstacle made the swimming path turn backward, while keeping the head in front, by about 100–240 degrees from the original swimming direction. We have demonstrated that this characteristic turning behaviour can be brought about by the combination of quiescence, straight path, and circular path. Analyses of stopping and starting transients of the quiescence (Gibbons and Gibbons, 1980b) show that the direction of the sperm changes by nearly 180 degrees during the stopping transient and that this new direction is kept during the starting transient; consequently the direction of the sperm changes by nearly 180 degrees.

After MS-induced quiescence, the sperm swims in the newly acquired direction for some distance. We showed that this process is associated with the straight path with more symmetrical flagellar beating. Our results that the symmetrical beating phase occurs at a higher than normal concentration of Ca^{2+} is not in accord with the general understanding that flagellar asymmetry, but not the symmetry,

increases with an increase of Ca^{2+} (Brokaw, 1979, 1991). Symmetrical flagellar beating at a higher than normal level of Ca^{2+} has also been reported in the chemotactic response of sperm (Wood *et al.*, 2003; Shiba *et al.*, 2008). How the intracellular Ca^{2+} concentration is regulated in flagella to produce symmetrical beating is one of the questions remaining. If the control of symmetrical flagellar waveforms depends on a gradual change of the Ca^{2+} level in the flagellum but not on the absolute Ca^{2+} level (Böhmer *et al.*, 2005), symmetrical beating could not be observed in the conventional reactivation procedure, in which demembranated sperm are reactivated at fixed Ca^{2+} concentrations.

Regulation of Ca^{2+} efflux

The Ca^{2+} concentration in flagella gradually decreases throughout the arrest phase and the straight path phase, and finally, in the circular path phase, it reaches the normal (original) level same as that before the avoiding response. Among candidate proteins that mediate Ca^{2+} efflux from cells, plasma membrane Ca^{2+} ATPases (suPMCA) and K^+ -dependent Na^+/Ca^{2+} exchangers (suNCKX) have been well characterized in sea urchin sperm (Su and Vacquier, 2002; Gunaratne, *et al.*, 2006). Their importance for the normal swimming of sperm has been suggested, because their blockers 5(6)-carboxyeosin (CE) and KB-R7943 inhibit the

sperm motility (Su and Vacquier, 2002; Gunaratne, *et al.*, 2006). How suPMCA and suNCKX are involved in the regulation of sperm motility, however, has not been elucidated.

In the present study, we showed that in the avoiding response there are two steps in which the Ca^{2+} level decreases, one from the arrest phase to the straight path phase (Q-S) and the other from the straight path phase to the circular path phase (S- C_A), which were respectively inhibited by the blockers of suPMCA and suNCKX. Inhibition of the suPMCA activity by 3 μM CE eliminated the straight path phase after the quiescence, indicating that the decrease of Ca^{2+} level from the arrest phase to the straight path phase (Q-S) is caused by the activity of suPMCA. Inhibition of suNCKX by 1 μM KB-R7943 induced a stoppage of beating with a straight waveform after a C_B -Q-S type response; and the C_B -Q type response never appeared even at the higher concentration of 1.5 μM . These results indicate that suNCKX is probably not activated at the exact quiescence state but is activated by the lower Ca^{2+} level than that at the quiescence, and that suNCKX triggers the Ca^{2+} efflux responsible for the step from the straight path phase to the circular path phase (S- C_A) (Fig. 5).

By mild inhibition of suPMCA at 1 μM CE, a unique C_B -Q- C_A type response was dominantly induced. A possible explanation for the induction of C_B -Q- C_A type response is that at the late arrest phase and/or at the straight path phase there is a threshold of the Ca^{2+} level for switching on the suNCKX activity. However, in the presence of 1 μM CE with 1 μM KB-R7943, which should facilitate the inhibition of Ca^{2+} efflux, thereby to increase the intracellular Ca^{2+} concentration, the C_B -Q type response was not induced. This indicates that there are no specific Ca^{2+} concentrations to switch on/off the activity of suPMCA and suNCKX. Another possible explanation would be that the progression of response from Q to C_A is triggered by the activity of suNCKX, in which we postulate that mild inhibition of the activity of suPMCA by 1 μM CE enhances the activity of suNCKX. This idea is supported by the observation that when 1 μM KB-R7943 was present in addition to 1 and 1.5 μM CE, the sperm stimulated by MS showed the C_B -Q-S type response and the C_B -Q-S- C_A type response in addition to the C_B -Q- C_A type response (Fig. 4E). In these cases, the activity of suNCKX dominates that of suPMCA. The responses in the presence of 2.5 μM CE with 1 μM KB-R7943 also support the idea. The proportion of the C_B -Q- C_A type response in the presence of 2.5 μM CE with 1 μM KB-R7943 was similar to that in the presence of 1 μM CE alone (Fig. 4C and E), indicating that the inhibition of suNCKX activity by KB-R7943 could be cancelled by enhancement of the suNCKX activity probably caused by 2.5 μM CE. It is likely that CE does not only inhibit the suPMCA activity to cause the disappearance of S phase but also enhances the suNCKX activity to produce the C_B -Q- C_A type response.

It is generally thought that PMCA binds Ca^{2+} with high

affinity but has relatively low turnover rates, typically $\sim 100 \text{ sec}^{-1}$, whereas $\text{Na}^+/\text{Ca}^{2+}$ exchanger has a 10-fold lower affinity for Ca^{2+} but 10- to 50-fold higher turnover rate than PMCA (Blaustein and Lederer, 1999). These basic properties of the two kinds of Ca^{2+} -dependent signaling proteins apparently disagree with the present result that the suPMCA functions at higher Ca^{2+} concentrations in the phase progression from Q to S, whereas the suNCKX functions at lower Ca^{2+} concentrations in the phase progression from S to C_A . The roles of suPMCA and suNCKX may be reversed in sea urchin sperm. As has been discussed above, however, the activity of suPMCA and suNCKX is not regulated solely by the intracellular Ca^{2+} concentration. There may be some interaction and combination in the regulation of the suPMCA and suNCKX activities, which enables the characteristic sequential changes of the Ca^{2+} concentration to induce the avoiding response of the sperm. The key process is the S phase, in which the Ca^{2+} concentration gradually decreases at a slow rate. For such regulation the function of suPMCA seems suitable. The presence of the Q phase in the high Ca^{2+} condition just before the S phase, however, makes the regulation more complex, because the release from the Q phase would require a Ca^{2+} efflux at a higher turnover rate, which could be achieved by the activity of suNCKX. Thus, the combination of the two kinds of proteins would be necessary for the progression of the avoiding response (Fig. 5). The mechanism regulating the combination is one of the questions remaining.

Flagelliasialin-related Ca^{2+} efflux system

Flagelliasialin has been suggested to be involved in the regulation of sperm motility, because in the presence of 4F7 sperm motility is inhibited and the Ca^{2+} level in the sperm flagella increases (Miyata *et al.*, 2004, 2006). These effects are very similar to the previously reported effects of CE and KB-R7943 (Su and Vacquier, 2002; Gunaratne, *et al.*, 2006). The present study using MS-induced avoiding responses has revealed that the flagelliasialin is involved in the regulation of the avoiding response by modulating a Ca^{2+} efflux system. 4F7 did not inhibit the response of the sperm to become quiescent, but inhibited the normal progression of response after the quiescence, inducing as a result the C_B -Q type response. These effects are apparently similar to those of CE. The stoppage of beating at the Q phase by 4F7 can also be explained as due to the increase of Ca^{2+} concentration caused by dysfunction of the voltage-dependent Ca^{2+} channels (Miyata *et al.*, 2006). If this is the case, the flagelliasialin-related Ca^{2+} control system (FLSCS) would reduce the Ca^{2+} influx and therefore the presence of 4F7 would possibly prolong the Q phase of C_B -Q-S- C_A . We found, however, the average duration of the arrest phase of C_B -Q-S- C_A (6–9 min, Fig. 4F) was not increased by 4F7 ($1.03 \pm 0.65 \text{ sec}$, $n=9$). It has been reported that glycoproteins related to the voltage-dependent Ca^{2+} channels contribute to

the amplification of Ca^{2+} influx (Gurnett *et al.*, 1996; Davies *et al.*, 2010), but their inhibitory role is unclear. At the present time, we are not able to conclude that the FLSCS is possibly involved in the regulation of the Ca^{2+} influx system.

It is tempting to speculate that flagelliasialin may modulate the suPMCA activity. In the present study, suPMCA appeared to lower the intracellular Ca^{2+} level in two steps, i.e. a decrease in the arrest phase (the inhibition of this step resulted in the $\text{C}_B\text{-Q}$ type response) and a further decrease to the level of the straight path phase (inhibition of this step resulted in the $\text{C}_B\text{-Q-C}_A$ type response with possible contribution of the suNCKX). In contrast, flagelliasialin seems to contribute to the decrease in Ca^{2+} levels from the quiescence state to the circular path state (inhibition of this step resulted in the $\text{C}_B\text{-Q}$ type response). Such a difference in the effects may be due to the different mechanisms of their function. Thus, the activity of suPMCA in the membrane is regulated by the conformational state of the two subunits coupled with ATP-hydrolysis at the cytosolic ATP-binding domain (Toyoshima *et al.*, 2000) and eosin inhibits its activity presumably by crossing the membrane (Gatto *et al.*, 1995), while the highly negative-charged flagelliasialin on the extracellular side of the membrane may similarly affect the positively charged amino acid residues of pores of Ca^{2+} transport proteins, as has been suggested in another type of polysialic acid for the AMPA-receptors (Vaithianathan *et al.*, 2004), and in the case of flagelliasialin the Ca^{2+} efflux activity is potentiated. 4F7 blocks such interaction between flagelliasialin and the Ca^{2+} efflux system.

Differences of localization may be another factor to be considered: suPMCA is suggested to be more concentrated in the sperm head plasma membrane than in the flagellar membrane (Gunaratne, *et al.*, 2006), whereas suNCKX localizes in the flagellar membrane (Su and Vacquier, 2002). Flagelliasialin is detected mainly in the flagellar membrane (Miyata *et al.*, 2004), although under immunofluorescent study flagelliasialin has also been detected in the head membrane (S. Miyata *et al.*, unpublished). At the present time we could not conclude whether flagelliasialin directly regulates the activity of suPMCA (Fig. 5). However, our observation that pretreatment of immotile sperm with 4F7 did not shorten the time necessary for inhibition of the MS-induced responses indicates that motility inhibition requires a certain response after the start of swimming. If the membrane Ca^{2+} transport proteins are rearranged after the initiation of swimming, it is possible to postulate that the swimming-dependent reaction time (about 5 min) is necessary for the movement of suPMCA from the sperm head membrane to the flagellar membrane (probably near the base of the flagellum) and/or for the movement in the head membrane. On the membrane, probably in lipid rafts (microenvironments) (Simons and Toomre, 2000), suPMCA would interact with flagelliasialin and contribute to stable Ca^{2+} efflux, because flagelliasialin is also localized in lipid

rafts (Miyata *et al.*, 2004). We could not exclude the possibility that the flagelliasialin also interacts with the suNCKX in the rafts of the flagellar membrane (Su and Vacquier, 2002) and regulates the suNCKX activity. For further understanding of the nature of the FLSCS as well as the mechanism of the flagelliasialin function, we need a more precise time-dependent analysis of the Ca^{2+} dynamics in the sperm head and flagellum.

Spontaneous Ca^{2+} entry and efflux during swimming

After a 10 min treatment with blockers and antibodies, we found that the swimming sperm showed a stoppage of beating with characteristic waveforms (quiescence for CE and 4F7, and a straight flagellum for KB-R7943), but, interestingly, this inhibition of beating could be rescued by a simultaneous addition of verapamil or Co^{2+} . This phenomenon probably relates to the spontaneous fluctuation of the resting membrane potential due to a small increase and a decrease in the intracellular Ca^{2+} concentration, reported in *Paramecium* (Nakaoka *et al.*, 2009). The present study revealed that, in the resting state (during normal swimming), the Ca^{2+} entry due to the activity of voltage-dependent Ca^{2+} channels is balanced with the Ca^{2+} efflux induced by the activity of suPMCA, FLSCS and suNCKX. Such Ca^{2+} fluctuation may function as an activating system of the Ca^{2+} channels in a “positive feedback manner” as suggested by Nakaoka *et al.* (2009) by probably tuning the Ca^{2+} at a higher level than the level without fluctuation. The fact that not only CE and KB-R7943 but also 4F7 is able to inhibit this Ca^{2+} fluctuation indicates that the function of the flagelliasialin-related Ca^{2+} control system is not additive but essential for the Ca^{2+} dependent regulation of sperm behaviour.

Our results show that the Ca^{2+} -dependent mechanosensitivity plays an important role in the swimming behaviour of the sea urchin sperm, and that the Ca^{2+} regulation in flagella is achieved by organized functioning of the membrane environment including voltage-dependent Ca^{2+} channels, plasma membrane Ca^{2+} ATPases, K^{+} -dependent $\text{Na}^{+}/\text{Ca}^{2+}$ exchangers and the flagelliasialin-related Ca^{2+} control system.

Acknowledgments. We would like to express our gratitude to Professor Keiichi Takahashi for discussion and suggestions for improving the manuscript. We thank Dr Ken-ichi Wakabayashi for technical advice and discussion. We also thank the Directors and staff of the Misaki Marine Biological Station, University of Tokyo, Education and Research Center for Marine Biology Asamushi, Tohoku University and Tateyama Marine Laboratory, Ochanomizu University for providing sea urchins. This work was supported in part by Grant-in-Aid for Scientific Research (B) and Grant-in-Aid for Scientific Research on Priority Areas from the MEXT, the Japanese Government (Nos. 22370028 and 21026006 for C. Shingyoji; Nos. 21370030 and 21026008 for M.Y.), Grants-in-Aid for Scientific Research (C) from the MEXT, the Japanese Government (No. 20570107 for C. Sato) and Hayashi Memorial Foundation for Female Natural Scientists (for C. Sato).

References

- Baba, S.A. and Mogami, Y. 1985. An approach to digital image analysis of bending shapes of eukaryotic flagella and cilia. *Cell Motility*, **5**: 475–489.
- Blaustein, M.P. and Lederer, W.J. 1999. Sodium/calcium exchange: Its physiological implications. *Physiol. Rev.*, **79**: 763–854.
- Böhmer, M., Van, Q., Weyand, I., Hagen, V., Beyermann, M., Matsumoto, M., Hoshi, M., Hildebrand, E., and Kaupp, U.B. 2005. Ca^{2+} spikes in the flagellum control chemotactic behavior of sperm. *EMBO J.*, **24**: 2741–2752.
- Brokaw, C.J., Josslin, R., and Bobrow, L. 1974. Calcium ion regulation of flagellar beat symmetry in reactivated sea urchin spermatozoa. *Biochem. Biophys. Res. Commun.*, **58**: 795–800.
- Brokaw, C.J. 1979. Calcium-induced asymmetrical beating of triton-demembrated sea urchin sperm flagella. *J. Cell Biol.*, **82**: 401–411.
- Brokaw, C.J. 1991. Calcium sensors in sea urchin sperm flagella. *Cell Motil. Cytoskeleton*, **18**: 123–130.
- Darszon, A., Beltrán, C., Felix, R., Nishigaki, T., and Treviño, C.L. 2001. Ion Transport in Sperm Signaling. *Dev. Biol.*, **240**: 1–14.
- Darszon, A., Acevedo, J.J., Galindo, B.E., Hernández-González, E.O., Nishigaki, T., Treviño, C.L., Wood, C., and Beltrán, C. 2006. Sperm channel diversity and functional multiplicity. *Reproduction*, **131**: 977–988.
- Davies, A., Kadurin, I., Alvarez-Laviada, A., Douglas, L., Nieto-Rostro, M., Bauer, C.S., Pratt, W.S., and Dolphin, A.C. 2010. The $\alpha_2\delta$ subunits of voltage-gated calcium channels form GPI-anchored proteins, a post-translational modification essential for function. *Proc. Natl. Acad. Sci. USA*, **107**: 1654–1659.
- Gatto, C., Hale, C.C., Xu, W., and Milanick, M.A. 1995. Eosin, a potent inhibitor of the plasma membrane Ca pump, does not inhibit the cardiac Na-Ca exchanger. *Biochemistry*, **34**: 965–972.
- Gibbons, B.H. and Gibbons, I.R. 1972. Flagellar movement and adenosine triphosphatase activity in sea urchin sperm extracted with Triton X-100. *J. Cell Biol.*, **54**: 75–97.
- Gibbons, B.H. 1980. Intermittent swimming in live sea urchin sperm. *J. Cell Biol.*, **84**: 1–12.
- Gibbons, B.H. and Gibbons, I.R. 1980a. Calcium-induced quiescence in reactivated sea urchin sperm. *J. Cell Biol.*, **84**: 13–27.
- Gibbons, I.R. and Gibbons, B.H. 1980b. Transient flagellar waveforms during intermittent swimming in sea urchin sperm. I. Wave parameters. *J. Muscle Res. Cell Motil.*, **1**: 31–59.
- Gunaratne, H.J., Neill, A.T., and Vacquier, V.D. 2006. Plasma membrane calcium ATPase is concentrated in the head of sea urchin spermatozoa. *J. Cell Physiol.*, **207**: 413–419.
- Gurnett, C.A., Waard, M.D., and Campbell, K.P. 1996. Dual function of the voltage-dependent Ca^{2+} channel $\alpha_2\delta$ subunit in current stimulation and subunit interaction. *Neuron*, **16**: 431–440.
- Ishikawa, R. and Shingyoji, C. 2007. Induction of beating by imposed bending or mechanical pulse in demembrated, motionless sea urchin sperm flagella at very low ATP concentrations. *Cell Struct. Funct.*, **32**: 17–27.
- Kaupp, U.B., Solzin, J., Hildebrand, E., Brown, J.E., Helbig, A., Hagen, V., Beyermann, M., Pampaloni, F., and Weyand, I. 2003. The signal flow and motor response controlling chemotaxis of sea urchin sperm. *Nature Cell Biol.*, **5**: 109–117.
- Krasznai, Z., Morisawa, M., Krasznai, Z.T., Morisawa, S., Inaba, K., Bazsáné, Z.K., Rubovszky, B., Bodnár, B., Borsos, A., and Márián, T. 2003. Gadolinium, a mechano-sensitive channel blocker, inhibits osmosis-initiated motility of sea- and freshwater fish sperm, but does not affect human or ascidian sperm motility. *Cell Motil. Cytoskeleton*, **55**: 232–243.
- Miyata, S., Sato, C., Kitamura, S., Toriyama, M., and Kitajima, K. 2004. A major flagellum sialoglycoprotein in sea urchin sperm contains a novel polysialic acid, an $\alpha_2,9$ -linked poly-*N*-acetylneuraminic acid chain, capped by an 8-*O*-sulfated sialic acid residue. *Glycobiology*, **14**: 827–840.
- Miyata, S., Sato, C., Kumita, H., Toriyama, M., Vacquier, V.D., and Kitajima, K. 2006. Flagelliasialin: a novel sulfated $\alpha_2,9$ -linked polysialic acid glycoprotein of sea urchin sperm flagella. *Glycobiology*, **16**: 1229–1241.
- Murakami, A. and Machemer, H. 1982. Mechanoreception and signal transmission in the lateral ciliated cell on the gills of *Mytilus*. *J. Comp. Physiol.*, **145**: 351–362.
- Naitoh, Y. and Kaneko, H. 1972. Reactivated Triton-extracted models of *Paramecium*: Modification of ciliary movement by calcium ions. *Science*, **176**: 523–524.
- Nakaoka, Y., Imaji, T., Hara, M., and Hashimoto, N. 2009. Spontaneous fluctuation of the resting membrane potential in *Paramecium*: amplification caused by intracellular Ca^{2+} . *J. Exp. Biol.*, **212**: 270–276.
- Ogura, A. and Takahashi, K. 1976. Artificial deciliation causes loss of calcium-dependent responses in *Paramecium*. *Nature*, **264**: 170–172.
- Ogura, A. and Machemer, H. 1980. Distribution of mechanoreceptor channels in the *Paramecium* surface membrane. *J. Comp. Physiol.*, **135**: 233–242.
- Ohta, K., Sato, C., Matsuda, T., Toriyama, M., Lennarz, W.J., and Kitajima, K. 1999. Isolation and characterization of low density detergent-insoluble membrane (LD-DIM) fraction from sea urchin sperm. *Biochem. Biophys. Res. Commun.*, **258**: 616–623.
- Okuno, M. and Hiramoto, Y. 1976. Mechanical stimulation of starfish sperm flagella. *J. Exp. Biol.*, **65**: 401–413.
- Rodríguez, E. and Darszon, A. 2003. Intracellular sodium changes during the speract response and the acrosome reaction in sea urchin sperm. *J. Physiol.*, **546**: 89–100.
- Shiba, K., Mogami, Y., and Baba, S.A. 2002. Ciliary movement of sea urchin embryos. *Natural Sci. Rep. Ochanomizu Univ.*, **53**: 49–54.
- Shiba, K., Márián, T., Krasznai, Z., Baba, S.A., Morisawa, M., and Yoshida, M. 2006. $\text{Na}^+/\text{Ca}^{2+}$ exchanger modulates the flagellar wave pattern for the regulation of motility activation and chemotaxis in the ascidian spermatozoa. *Cell Motil. Cytoskeleton*, **63**: 623–632.
- Shiba, K., Baba, S.A., Inoue, T., and Yoshida, M. 2008. Ca^{2+} bursts occur around a local minimal concentration of attractant and trigger sperm chemotactic response. *Proc. Natl. Acad. Sci. USA*, **105**: 19312–19317.
- Shingyoji, C. and Takahashi, K. 1995. Flagellar quiescence response in sea urchin sperm induced by electric stimulation. *Cell Motil. Cytoskeleton*, **31**: 59–65.
- Shingyoji, C., Yoshimura, K., Eshel, D., Takahashi, K., and Gibbons, I.R. 1995. Effect of beat frequency on the velocity of microtubule sliding in reactivated sea urchin sperm flagella under imposed head vibration. *J. Exp. Biol.*, **198**: 645–653.
- Simons, K. and Toomre, D. 2000. Lipid rafts and signal transduction. *Nature Rev. Mol. Cell Biol.*, **1**: 31–39.
- Su, Y.H. and Vacquier, V.D. 2002. A flagellar K^+ -dependent $\text{Na}^+/\text{Ca}^{2+}$ exchanger keeps Ca^{2+} low in sea urchin spermatozoa. *Proc. Natl. Acad. Sci. USA*, **99**: 6743–6748.
- Toyoshima, C., Nakasako, M., Nomura, H., and Ogawa, H. 2000. Crystal structure of the calcium pump of sarcoplasmic reticulum at 2.6 Å resolution. *Nature*, **405**: 647–655.
- Vaithianathan, T., Matthias, K., Bahr, B., Schachner, M., Suppiramaniam, V., Dityatev, A., and Steinhäuser, C. 2004. Neural cell adhesion molecule-associated polysialic acid potentiates α -amino-3-hydroxy-5-methylisoxazole-4-propionic acid receptor currents. *J. Biol. Chem.*, **279**: 232–243.

- 47975–47984.
- Wakabayashi, K., Ide, T., and Kamiya, R. 2009. Calcium-dependent flagellar motility activation in *Chlamydomonas reinhardtii* in response to mechanical agitation. *Cell Motil. Cytoskeleton*, **66**: 736–742.
- Wood, C.D., Darszon, A., and Whitaker, M. 2003. Speract induces calcium oscillations in the sperm tail. *J. Cell Biol.*, **161**: 89–101.
- Wood, C.D., Nishigaki, T., Furuta, T., Baba, S.A., and Darszon, A. 2005. Real-time analysis of the role of Ca^{2+} in flagellar movement and motility in single sea urchin sperm. *J. Cell Biol.*, **169**: 725–731.
- Yamakawa, N., Sato C., Miyata, S., Maehashi, E., Toriyama, M., Sato, N., Furuhashi, K., and Kitajima, K. 2007. Development of sensitive chemical and immunochemical methods for detecting sulfated sialic acids and their application to glycoconjugates from sea urchin sperm and eggs. *Biochimie*, **89**: 1396–1408.
- Yang, X.C. and Sachs, F. 1989. Block of stretch-activated ion channels in *Xenopus* oocytes by gadolinium and calcium ions. *Science*, **243**: 1068–1071.
- Yoshimura, K. 1996. A novel type of mechanoreception by the flagella of *Chlamydomonas*. *J. Exp. Biol.*, **199**: 295–302.

(Received for publication, November 1, 2010, accepted, January 7, 2011
and published online, February 25, 2011)